Rydberg atoms in magnetic quadrupole traps

EUROPHYSICS LETTERS 15 February 2004

Europhys. Lett., **65** (4), pp. 478–484 (2004)
DOI: 10.1209/epl/i2003-10109-0

Rydberg atoms in magnetic quadrupole traps

I. LESANOVSKY[1](*), J. SCHMIEDMAYER[1](**) and P. SCHMELCHER[1,2](***)

[1] *Physikalisches Institut, Universität Heidelberg*
Philosophenweg 12, 69120 Heidelberg, Germany
[2] *Theoretische Chemie, Institut für Physikalische Chemie, Universität Heidelberg*
INF 229 - 69120 Heidelberg, Germany

(received 22 October 2003; accepted in final form 2 December 2003)

PACS. 31.15.-p – Calculations and mathematical techniques in atomic and molecular physics (excluding electron correlation calculations).
PACS. 32.60.+i – Atomic properties and interactions with photons: Zeeman and Stark effects.
PACS. 33.55.Be – Molecular properties and interactions with photons: Zeeman and Stark effects.

Abstract. – We investigate the electronic structure and properties of Rydberg atoms exposed to a magnetic quadrupole field. It is shown that the spatial as well as generalized time-reversal symmetries lead to a two-fold degeneracy of the electronic states in the presence of the external field. A delicate interplay between the Coulomb and magnetic interactions in the inhomogeneous field leads to an unusual weak field splitting of the energy levels as well as complex spatial patterns of the corresponding spin polarization density of individual Rydberg states. Remarkably, the magnetic quadrupole field induces a permanent electric-dipole moment of the atom.

The past two decades have seen substantial progress of our knowledge on highly excited Rydberg atoms exposed to homogeneous magnetic fields, providing major impact on areas such as quantum chaos, semiclassics of nonintegrable systems and properties of magnetized structures [1–4]. However, so far there exist no investigations on Rydberg atoms in inhomogeneous and/or trapping magnetic-field configurations. Apart from being of fundamental interest, trapped Rydberg atoms have recently been proposed to serve as a tool for quantum information processing in mesoscopic atomic ensembles [5]. For these applications the atoms have to be localized in sufficiently tight traps providing the appropriate confinement of the highly excited Rydberg states. Such a tight confinement can be achieved for neutral atoms in magnetic traps on atom chips [6], where large field gradients $\mathcal{B} \approx 10^8 \frac{\mathrm{G}}{\mathrm{cm}}$ are accessible. As a prototype example we study here the magnetic quadrupole field [7] that is a key element of magnetic trapping([1]). We show that Rydberg atoms confined to a quadrupole field possess a specific structure and symmetry that lead to twofold degeneracies of its eigenstates.

(*) E-mail: ilesanov@physi.uni-heidelberg.de
(**) E-mail: joerg.schmiedmayer@physi.uni-heidelberg.de
(***) E-mail: Peter.Schmelcher@pci.uni-heidelberg.de
([1])The quadrupole field is not a complete trap in itself.

The Rydberg states exhibit unique phenomena such as complex spin polarization patterns and magnetic-field–induced giant electric-dipole moments that can be understood by employing the underlying symmetries and analyzing the interplay between the Coulomb and magnetic interactions. We utilize a one-body approach for the Rydberg atom, where the motion of the excited outermost electron takes place in the field of a singly positive charged core. The accuracy of this assumption increases with increasing degree of excitation and holds particularly well for the frequently used alkali atoms which possess a single valence electron outside a closed shell core([2]). We assume that the atomic center of mass (CM) is localized at the center of the quadrupole field requiring an ultracold CM motion of the atom. The Hamiltonian $\mathcal{H} = \mathcal{H}_1 + \mathcal{H}_2$ in the presence of the quadrupole field $\vec{B}(\vec{r}) = \mathcal{B}(x, y, -2z)$ with the vector potential $\vec{A}(\vec{r}) = \frac{1}{3}[\vec{B}(\vec{r}) \times \vec{r}]$ reads

$$\begin{aligned}
\mathcal{H}_1 &= -\frac{\hbar^2}{2m_e}\left(\frac{\partial^2}{\partial r^2} + \frac{2}{r}\frac{\partial}{\partial r} + \frac{1}{r^2}\left\{\cot\theta\frac{\partial}{\partial\theta} + \frac{\partial^2}{\partial\theta^2}\right\} + \right. \\
&+ \left.\frac{1}{r^2\sin^2\theta}\frac{\partial^2}{\partial\phi^2}\right) - \frac{1}{4\pi\epsilon_0}\frac{e^2}{r} + i\frac{\hbar e}{m_e}\mathcal{B}r\cos\theta\frac{\partial}{\partial\phi} + \\
&+ \frac{e^2}{2m_e}\mathcal{B}^2r^4\cos^2\theta\sin^2\theta, \\
\mathcal{H}_2 &= \mu_{\mathrm{B}}\mathcal{B}r\big(\sin\theta\big\{\sigma_x\cos\phi + \sigma_y\sin\phi\big\} - 2\sigma_z\cos\theta\big). \qquad (1)
\end{aligned}$$

We have employed spherical coordinates. $\sigma_i (i = x, y, z)$ are the Pauli matrices acting in spin space. Here $\mathcal{B}$, μ_{B} are the field gradient and Bohr magneton, respectively. $\mathcal{H}_1$ contains the Coulomb, paramagnetic and diamagnetic interactions, whereas $\mathcal{H}_2$ contains the interaction of the spin with the magnetic field. Compared to the case of a homogeneous field, the Hamiltonian $\mathcal{H}$ exhibits a number of major differences. Depending on the value of the field gradient $\mathcal{B}$, it possesses a strong variability with respect to the appearance of its energy surfaces. The paramagnetic term ($\propto \mathcal{B}$) is, apart from its proportionality with respect to the angular momentum $L_z = \frac{\hbar}{i}\frac{\partial}{\partial\phi}$, additionally depending on the z-coordinate, and the diamagnetic interaction ($\propto \mathcal{B}^2$) represents an oscillator coupling term of fourth order for the motion perpendicular and parallel to the z-axis (see $\mathcal{H}_1$). In addition, $\mathcal{H}_2$ results in an intricate coupling of the spatial and spin electronic degrees of freedom via the inhomogeneity of the field. It is possible to eliminate the ϕ-dependence of the Hamiltonian $\mathcal{H}$ by applying the unitary transformation

$$U = \frac{1}{\sqrt{2}}\begin{pmatrix} -e^{-i\phi} & e^{-i\phi} \\ 1 & 1 \end{pmatrix} \qquad (2)$$

acting in spin and angular space. This is due to the rotational symmetry associated with the conservation of the total angular momentum $J_z = L_z + S_z$ possessing half-integer eigenvalues M. This conservation reflects the axial symmetry of the quadrupole field. The eigenfunctions of J_z (and $\mathcal{H}$) take the appearance $|\Phi_m\rangle = (\Phi^u(r,\theta)e^{i(m-1)\phi}, \Phi^d(r,\theta)e^{im\phi})$ with $M = m - \frac{1}{2}$, m being integer, and where $\Phi^{u,d}$ are the upper and lower components of the spinor, respectively. A close inspection of $\mathcal{H}$ yields a further spatial (unitary) symmetry $P_\phi O P_z$ that consists of the spatial z-parity operation P_z followed by an interchange $O(=\sigma_x)$ of the spin components and the ϕ-parity $P_\phi : \phi \to 2\pi - \phi$ operation. Additionally, $\mathcal{H}$ possesses the generalized time-reversal symmetry TOP_z, *i.e.* $[TOP_z, \mathcal{H}] = 0$, where T is the conventional time-reversal operation. $P_\phi O P_z$ and TOP_z do not commute with J_z but yield,

([2])Also, for excited states the spin-orbit and hyperfine interactions can be neglected due to their rapid drop-off with increasing energetical degree of excitation.

e.g., $[TOP_z, J_z] = (-2J_z)TOP_z$. Eigenfunctions to the TOP_z-operator are provided by the corresponding linear combination $|\Psi_m^{\pm}\rangle = \frac{1}{\sqrt{2}}[|\Phi_m\rangle \pm TOP_z|\Phi_m\rangle]$ with $TOP_z|\Psi_m^{\pm}\rangle = \pm|\Psi_m^{\pm}\rangle$. Beyond the above we have the additional symmetry operation TP_ϕ that commutes with both the Hamiltonian $\mathcal{H}$ and the angular momentum J_z. Employing $\{TOP_z, J_z\} = 0$ it can be shown that each energy eigenvalue is doubly degenerate with the two energy eigenstates being $|\Phi_m\rangle, |\Phi_m\rangle' = TOP_z|\Phi_m\rangle$, *i.e.* they possess the eigenvalues $\pm M$ with respect to J_z. The underlying symmetry group is non-Abelian and a semi-direct product $C_{\infty v} = C_\infty \bigotimes C_s$. This is in contrast to the case of a homogeneous magnetic field, where L_z, P_z, P, $T\sigma_z P_\phi$ constitute the spatial and time-reversal symmetries, respectively, and form an Abelian group thereby not causing any degeneracies due to symmetry. The above symmetries and degeneracies have to be carefully distinguished from the twofold Kramers degeneracy of spin-$\frac{1}{2}$ systems in the absence of the field. The latter is lifted if an external (even homogeneous) field is switched on. The degeneracies found here are due to the particular geometry of the quadrupole magnetic field. To investigate the electronic structure of the atom exposed to the field in detail we expand the eigenfunctions of $\mathcal{H}$ in two-component spinors according to

$$\Psi(r,\theta,\phi) = \sum_{n,l,\tilde{n},\tilde{l}} c_{n,l,\tilde{n},\tilde{l}} \begin{pmatrix} R_n^{(\zeta,k)}(r) Y_l^{(m-1)}(\theta,\phi) \\ R_{\tilde{n}}^{(\zeta,k)}(r) Y_{\tilde{l}}^{(m)}(\theta,\phi) \end{pmatrix}, \tag{3}$$

where (r,θ,ϕ), $Y_l^{(m)}$ are spherical coordinates and the spherical harmonics, respectively, and $R_n^{(\zeta,k)}(r) = \sqrt{\frac{n!}{(n+2k)!}} e^{-\frac{\zeta r}{2}} (\zeta r)^k L_n^{2k}(\zeta r)$ with L_n^a being the associated Laguerre polynomials. ζ is a nonlinear variational parameter to be optimized. We apply the energy variational principle linearly optimizing the coefficients $c_{n,l,\tilde{n},\tilde{l}}$ by solving the corresponding generalized eigenvalue problem (GEP). The Hamiltonian and overlap matrices can be calculated analytically possessing a band and block structure, respectively, that can be exploited in solving the GEP. Our approach to diagonalize the GEP consists of a Krylov-space approach using the Arnoldi-decomposition and furthermore applying a shift-and-invert procedure [8, 9]. This allows us to accurately describe highly excited states since the shift-and-invert approach combined with an optimized value for the parameter ζ ($\frac{2\sqrt{|E|}}{0.775}$ is a good choice) allows to converge the eigenvalues in a preselected window of the excitation energy. For the field gradients up to $\mathcal{B} = 10^{13}\,\frac{\mathrm{G}}{\mathrm{cm}}$ we have studied excitation spectra corresponding to the magnetic quantum numbers $M = (-\frac{7}{2}) - (+\frac{7}{2})$. For the gradients presently accessible for atom chips ($\mathcal{B} \leq 10^7\,\frac{\mathrm{G}}{\mathrm{cm}}$) all Rydberg states up to $n \approx 60$ (n refers to the corresponding field-free principal quantum number which is not a good quantum number in the presence of the field but serves as an energetical label) could be calculated with high accuracy. To investigate the properties of the excited states in more detail, we analyzed the spectrum $E_i(\mathcal{B})$ (i-th energy curve), the spatial probability densities $W_\Lambda(r,\theta) = r^2 \sin\theta |\Phi_m(r,\theta)|^2$ of individual states, the z-component of the spatial spin density $W_S(r,\theta) = \frac{\hbar}{2} \frac{|\Phi^u(r,\theta)|^2 - |\Phi^d(r,\theta)|^2|}{|\Phi^u(r,\theta)|^2 + |\Phi^d(r,\theta)|^2|}$ as well as several relevant expectation values such as dipole moments and spin polarizations. Emerging from $\mathcal{B} = 0$, we encounter for weak gradients a splitting of the degenerate energy levels that looks quite different from what is observed in the case of a homogeneous magnetic field. Focusing, *e.g.*, on $M = \frac{1}{2}$ and a given n-manifold, the splitting in a homogeneous field takes place into two bundles, each consisting of almost degenerate n and $n-1$ sublevels (see inset of fig. 1a), respectively. One of the bundles is (approximately) independent of the field and the other one raises linearly with increasing field strength. In the quadrupole field the degenerate n-manifold of $M = \frac{1}{2}$-states splits into its $2n-1$ components, *i.e.* energy curves $E_i(\mathcal{B})$ (see fig. 1a). Each curve behaves approximately linear with increasing field gradient (in the weak gradient regime where the

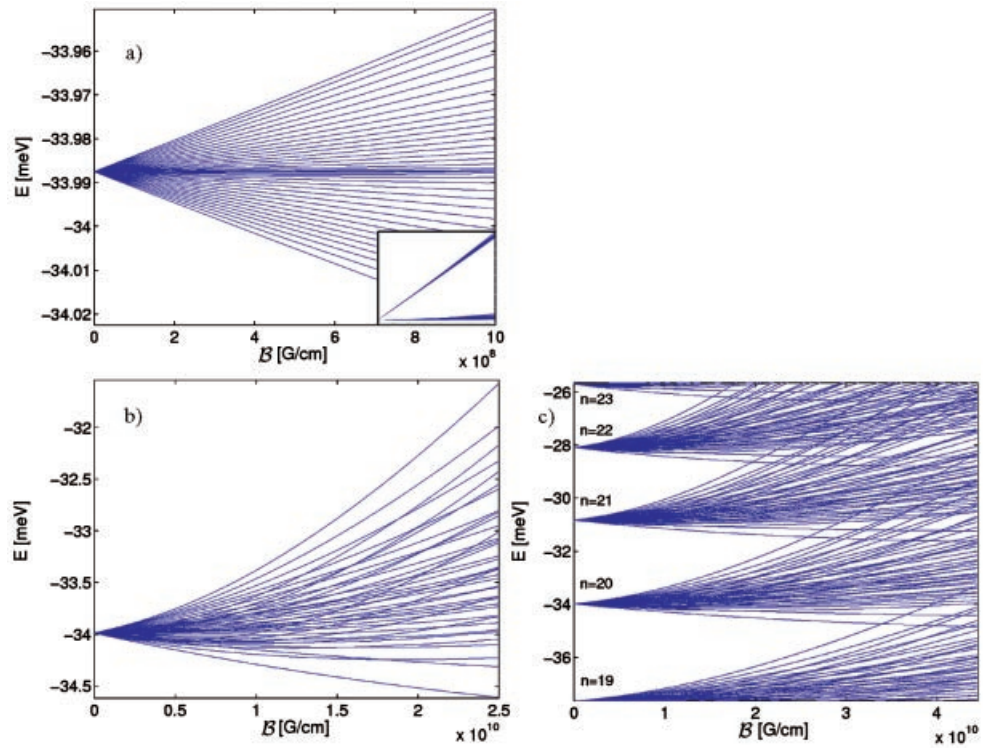

Fig. 1 – a) Symmetric linear splitting of the 39 (for $\mathcal{B} = 0$) degenerate energy levels belonging to the multiplett $n = 20$, $m = 1$ for weak gradients. Inset: The splitting of the same states in a homogeneous magnetic field covering the range $0 \leq B \leq 0.235$ Tesla. b) The splitting of the same multiplett for a larger range of field gradients covering the regime of l-mixing. Very narrow avoided crossings occur in this regime. c) The energy levels as a function of the field gradient $\mathcal{B}$ emerging for the $n = 19$–23, $M = \frac{1}{2}$ manifolds. The inter n-manifold mixing for strong gradients is clearly visible.

paramagnetic interaction dominates) but possesses a different slope. The curves $E_i(\mathcal{B})$ are arranged symmetrically with respect to the constant $E_i(0)$, as can be seen in fig. 1. With increasing $\mathcal{B}$ the clusters of levels widen further and the curves $E_i(\mathcal{B})$ become nonlinear (see fig. 1b). The field gradient for intra n-manifold mixing of different angular momentum, *i.e.* l-states, can be shown to scale as $\mathcal{B} \propto n^{-6}$. In this regime very narrow avoided crossings occur. With further increasing field gradient, the n-manifolds start to overlap (see fig. 1c) and we encounter inter n-manifold mixing that scales according to $\mathcal{B} \propto n^{-\frac{11}{2}}$ (in a homogeneous field the corresponding scaling for inter n-manifold mixing is $B \propto n^{-\frac{7}{2}}$). In this regime, the diamagnetic interaction of $\mathcal{H}_1$ is important and no (not even approximate) symmetries remain. Level repulsion and avoided crossings are therefore a characteristic feature of the spectrum. In the quadrupole field the spatial probability distributions of the J_z-eigenstates are typically localized in one half-volume either above or below the (x, y)-plane (see left column of fig. 2 which shows the distributions for the 15th and 76th excited state for $\mathcal{B} = 4.4 \cdot 10^9 \frac{\mathrm{G}}{\mathrm{cm}}$)([3]). With increasing degree of excitation of the eigenstates, the diamagnetic interaction becomes important and leads to an additional deformation of the electronic probability density. In

([3])This property is related to the existence of permanent electric-dipole moments, as discussed below.

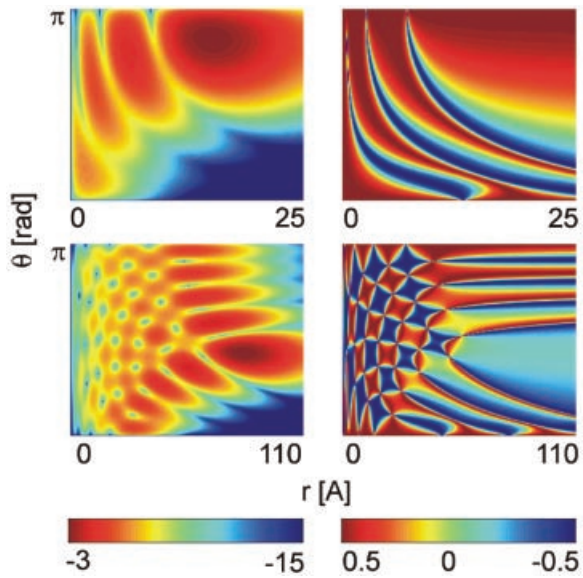

Fig. 2 – The spatial probability density W_Λ (left column, logarithmic representation) together with the S_z-density in r, θ-space (right column) for the 15th excited state with $M = \frac{1}{2}$ for $\mathcal{B} = 4.4 \cdot 10^9 \frac{\mathrm{G}}{\mathrm{cm}}$ (upper panel) and for the 76th excited state (lower panel) emerging from $n = 9$ with $M = \frac{1}{2}$ for the same gradient. The asymmetry of the probability density with respect to the line $\theta = \frac{\pi}{2}$, *i.e.* for $z \to -z$, is clearly visible.

a homogeneous magnetic field z-parity is a symmetry and W_Λ is symmetric with respect to reflections at the (x, y)-plane. Considering the expectation value $\langle r \rangle$ for the states with increasing n, the effect of the quadrupole field is twofold: it modifies the distribution of $\langle r \rangle$ values within a single n-manifold and decreases the center of the distribution due to the compression of the electronic cloud in the quadrupole field. Looking at the spatial W_S-spin density of the electronic states some remarkable properties appear. Figure 2 shows $W_S(r, \theta)$ for the 15th and 76th excited state for a field gradient $\mathcal{B} = 4.4 \cdot 10^9 \frac{\mathrm{G}}{\mathrm{cm}}$. For the 15th excited state, W_S shows curved stripes of upward and downward polarized spin, respectively, that match with the regions of the localization of the spatial probability density W_Λ. For the 76th excited state, a pattern of nested islands appears with each island possessing a certain spin polarization and well-localized transition regions separating them. These islands correspond to locally either upward- or downward-pointing spin and are arranged in a chessboard-like pattern. The borderlines between the islands correspond to a vanishing z-component of the spin. The intersection of the borderlines, *i.e.* the corners of the islands, represent the nodes of the spatial probability densities of the Rydberg states, as can be seen from the corresponding graph W_Λ in fig. 2. With increasing value of r, the shape of the islands becomes elongated in radial direction and finally turns into directed stripes with continuous transitions of the spin polarization. The formation of the islands is due to a detailed balance of the interactions in the Hamiltonian $\mathcal{H}$. This does not occur for the atom in a homogeneous magnetic field (constant spin polarization) nor for the case of a pure spin in a quadrupole magnetic field described by $\mathcal{H}_2$ only. The latter yields a spin polarization density that is independent of r showing horizontal stripes in the (r, θ)-representation of W_S. These stripes can be found for W_S of the Rydberg states in fig. 2 for large values of r in a modified form indicating the dom-

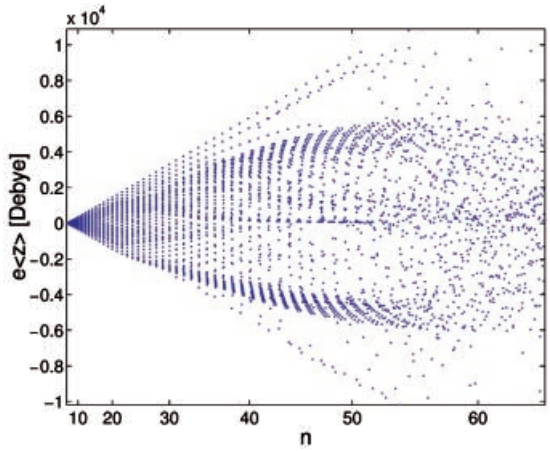

Fig. 3 – The expectation value of the electric dipole moment along the z-axis for $\mathcal{B} = 4.4 \cdot 10^8 \frac{\mathrm{G}}{\mathrm{cm}}$ for the states with $M = \frac{1}{2}$. n labels the excitation energy.

inance of the spin coupling to the magnetic field in this regime. Analyzing the spin density of many states, we found that the above behaviour is generic. The spin polarization patterns are features of individual electronic eigenstates and become increasingly more detailed with increasing degree of excitation of the state considered. Transitions among eigenstates to the total angular momentum J_z obey the selection rules $\Delta M = 0$ and $\Delta M = \pm 1$ for dipole transitions via linearly and circularly polarized light, as is the case without the presence of the field. Linearly z-polarized transitions between TOP_z-eigenstates must involve states with different TOP_z symmetries in order to possess a nonvanishing dipole strength. The fact that the quadrupole field causes a nonsymmetric charge distribution with respect to the horizontal (x, y)-plane leads to the following peculiar properties of the atom: Electronic eigenstates to J_z possess a nonvanishing permanent electric-dipole moment $e\langle z\rangle$ only along the symmetry axis of the quadrupole field, *i.e.* the external magnetic field induces a permanent electric-dipole moment of the atom. Figure 3 illustrates the distribution of dipole moments for a variety of states belonging to the manifolds $n \leq 65$. The variance of the distribution of dipole moments increases strongly with increasing degree of excitation n, thereby showing a transition from a regular alignment to an irregular spreading. In a homogeneous magnetic field the deformation of the charge distribution is (due to parity symmetry) such that the electric-dipole moment vanishes. One possibility to probe the above-described properties of Rydberg atoms in quadrupole magnetic fields would be to perform spectroscopy of single atoms in traps on, preferably, atom chips, since these possess currently the strongest available field gradients. This would provide us with detailed information on the level splitting and evolution with increasing degree of excitation.

Already in the presence of a homogeneous magnetic field it is well-known that the CM and electronic motion of an atom do not decouple [10–12]. To enter the corresponding regime where the residual coupling becomes important certain parameter values (excitation energy, CM energy, etc.) have to be addressed. A variety of intriguing phenomena due to the mixing of the internal and CM motion such as the diffusion of the CM or giant dipole states are then observed [13–15]. In the quadrupole field the assumption that the atom is ultracold will certainly minimize the CM motional effects. Nevertheless, a residual coupling is unavoidable and its impact on the electronic structure is, at this point, simply unknown: A full treatment of

the two-body system certainly goes beyond the scope of the present investigation and requires, both from the conceptual as well as computational point of view, major investigations. On the other hand, one should note that the symmetries discussed here equally hold for the moving two-body system, *i.e.* the total angular momentum is conserved and the unitary as well as antiunitary spin-spatial symmetries, now applied to both particles, are also present.

Beyond the above, one can speculate about potential applications of the magnetic-field–induced permanent electric-dipole moments of the atoms. Populating with a laser excited states with a desired dipole moment for certain atoms within an array of single atom traps can open the route to a controlled interaction between the atoms which is currently of major interest for quantum information processing [5, 16–18].

* * *

Discussions with O. Alon and M. Anderson are gratefully acknowledged. JS acknowledges financial support by the European Union contract numbers IST-2001-38863 (ACQP).

REFERENCES

[1] Friedrich H. and Wintgen D., *Phys. Rep.*, **183** (1989) 37.
[2] Ruder H. *et al.*, *Atoms in Strong Magnetic Fields* (Springer) 1992.
[3] Friedrich H. and Eckhardt B. (Editors), *Classical, Semiclassical and Quantum Dynamics in Atoms*, *Lect. Notes Phys.*, Vol. **485** (Springer-Verlag, Heidelberg) 1997.
[4] Schmelcher P. and Schweizer W. (Editors), *Atoms and Molecules in Strong External Fields* (Plenum Press) 1998.
[5] Lukin M. D. *et al.*, *Phys. Rev. Lett.*, **87** (2001) 037901.
[6] Folman R. *et al.*, *Adv. At. Mol. Opt. Phys.*, **48** (2002) 263.
[7] Bergeman T. H. *et al.*, *J. Opt. Soc. Am. B*, **6** (1989) 2249.
[8] Sorensen D. C., *Implicitly restarted Arnoldi/Lanczos methods for large scale eigenvalue calculations*, in *Parallel Numerical Algorithms*, edited by Keyes D. E., Sameh A. and Venkatakrishnan V. (Kluwer, Dordrecht) 1995.
[9] Demmel J. W., Gilbert J. R. and Xiaoye Li S., *SuperLU Users' Guide* (University of California, Berkeley) 1999.
[10] Avron J., Herbst I. and Simon B., *Ann. Phys. (N.Y.)*, **114** (1978) 431.
[11] Johnson B., Hirschfelder J. and Yang K., *Rev. Mod. Phys.*, **55** (1983) 109.
[12] Schmelcher P., Cederbaum L. S. and Kappes U., *Conceptual Trends in Quantum Chemistry* (Kluwer Academic Publisher, Dordrecht) 1994, pp. 1-51.
[13] Schmelcher P. and Cederbaum L. S., *Phys. Lett. A*, **164** (1992) 305.
[14] Dippel O., Schmelcher P. and Cederbaum L. S., *Phys. Rev. A*, **49** (1994) 4415.
[15] Schmelcher P., *Phys. Rev. A*, **52** (1995) 130.
[16] Jaksch D. *et al.*, *Phys. Rev. Lett.*, **82** (1999) 1975.
[17] Calarco T. *et al.*, *Phys. Rev. A*, **61** (2000) 022304.
[18] Eckert K. *et al.*, *Phys. Rev. A*, **66** (2002) 042317.